Water Research 146 (2018) 146–158

Contents lists available at ScienceDirect

Water Research

journal homepage: www.elsevier.com/locate/watres

Influence of dissolved organic matter (DOM) characteristics on dissolved mercury (Hg) species composition in sediment porewater of lakes from southwest China

Tao Jiang [a, b], Andrea G. Bravo [c], Ulf Skyllberg [b], Erik Björn [d], Dingyong Wang [a], Haiyu Yan [e, *], Nelson W. Green [f]

[a] Department of Environment Science and Engineering, College of Resources and Environment, Southwest University, Chongqing, 400716, China
[b] Department of Forest Ecology and Management, Swedish University of Agricultural Sciences, Umeå SE-90183, Sweden
[c] Department of Environmental Chemistry, Institute of Environmental Assessment and Water Research (IDAEA), Spanish National Research Council (CSIC), Barcelona, 08034, Spain
[d] Department of Chemistry, Umeå University, SE-901-87, Umeå, Sweden
[e] State Key Laboratory of Environmental Geochemistry, Institute of Geochemistry, Chinese Academy of Sciences, Guiyang 550002, China
[f] School of Chemical and Biomolecular Engineering, Atlanta, GA, 30332, United States

ARTICLE INFO

Article history:
Received 7 March 2018
Received in revised form
20 August 2018
Accepted 25 August 2018
Available online 3 September 2018

Keywords:
Dissolved organic matter
Mercury
Methylmercury
Lake porewater
Sediment
Characterization

ABSTRACT

The origin and composition of dissolved organic matter (DOM) in porewater of lake sediments is intricate and decisive for fate of pollutants including mercury (Hg). While there are many reports on the relationship between dissolved organic carbon concentration (DOC) and mercury (Hg) concentrations in aquatic systems, there are few in which DOM compositional properties, that may better explain the fate of Hg, have been the focus. In this study, porewaters from sediments of three lakes, Caihai Lake (CH), Hongfeng Lake (HF) and Wujiangdu Lake (WJD), all located in southwest China, were selected to test the hypothesis that DOM optical properties control the fate of Hg in aquatic ecosystems. Porewater DOM was extracted and characterized by UV–Vis absorption and fluorescence spectroscopy. A two end-member (autochthonous and allochthonous DOM) mixing model was used to unveil the origin of DOM in porewaters of the three lakes. Our results show a higher input of terrestrial DOM in the pristine lake CH, as compared to lakes HF and WJD lakes, which were both influenced by urban environments and enriched in autochthonous DOM. While the relationships between the concentrations of DOC and the different chemical forms of Hg forms were quite inconsistent, we found important links between specific DOM components and the fate of Hg in the three lakes. In particular, our results suggest that allochthonous, terrestrial DOM inhibits Hg(II) availability for Hg methylating micro-organisms. In contrast, autochthonous DOM seems to have been stimulated MeHg formation, likely by enhancing the activity of microbial communities. Indeed, DOM biodegradation experiments revealed that differences in the microbial activity could explain the variation in the concentration of MeHg. While relationships between concentrations of DOC and Hg vary among different sites and provide little information about Hg cycling, we conclude that the transport and transformation of Hg (e.g. the methylation process) are more strongly linked to DOM chemical composition and reactivity.

1. Introduction

Dissolved organic matter (DOM) plays an important role in many biogeochemical processes including the global carbon cycle and fate of pollutants (e.g., trace heavy metals and organic containments) (Aiken et al., 2011a; b; Bolan et al., 2011; Nelson and Siegel, 2013; Mopper et al., 2015). As an important fraction of natural organic matter (Aiken et al., 2011b; Mostofa et al., 2013),

Abbreviations: BIX, Biological Index; CDOM, Chromophoric Dissolved Organic Matter; CVAFS, Cold Vapor Atomic Fluorescence Spectroscopy; DMeHg, Dissolved Methylmercury; DOC, Dissolved Organic Carbon; DOM, Dissolved Organic Matter; DTHg, Dissolved Total Mercury; EEMs, Excitation-Emission Matrices; FI, Fluorescence Index; HDOC, Hydrophobic Dissolved Organic Carbon; Hg, Mercury; MeHg, Methylmercury; NOM, Natural Organic Matter; OM, Organic Matter; THg, Total Mercury; SUVA, Specific Ultraviolet Absorbance; UV–Vis, Ultraviolet–Visible.

* Corresponding author.
E-mail address: yanhaiyu@vip.skleg.cn (H. Yan).

https://doi.org/10.1016/j.watres.2018.08.054
0043-1354/

DOM is widely recognized as a key environmental parameter, influencing the ecology of both aquatic and terrestrial environments (Tranvik et al., 2009; Aiken et al., 2011a; b). Sediments may function as a sink or source of natural organic matter and many types of pollutants (Förstner, 2004), including Hg (Isidorova et al., 2016). Pollutants are released from sediment particles into its porewater through desorption and dissolution processes, as well as by biological decomposition of NOM. Linking sediments to overlying water, DOM has a key role in the transfer of pollutants from sediments to the water column (Ziegelgruber et al., 2013; Abbott et al., 2015). Determination of porewater DOM characteristics in sediment and water is one of the fundamentals to improve our understanding of how DOM structures and DOM reactivity influence the fate of pollutants in the aquatic environment (Chen and Hur, 2015). The recent advancement of DOM characterization (Leenheer and Croué, 2003), UV–Vis and excitation-emission matrices (EEMs) fluorescence spectroscopy provides convenient and powerful tools to analyze DOM composition, widely used to track sources of DOM (e.g., autochthonous versus allochthonous) and DOM processing (Fellman et al., 2010; Coble et al., 2014). Because spectral characteristics of DOM in porewater can be used to track the composition and origin of DOM in the bulk sediment (Bravo et al., 2017), and reflect the microbial activity by its composition (Ziegelgruber et al., 2013), they have been proven useful tools for explaining the environmental fates of contaminants, such as mercury (Herrero Ortega et al., 2017; Kim et al., 2017; Lescord et al., 2018).

Mercury (Hg) contamination is a global environmental issue stemming from the severe damage it may cause humans and ecosystem health. Its methylated chemical form, methylmercury (MeHg), is of special concern because it accumulates in aquatic food webs through biomagnification processes (Lavoie et al., 2013; Lehnherr, 2014). The methylation of inorganic Hg, henceforth denoted Hg(II), to MeHg occurs under oxygen-limited conditions such as those found in submerged soils (e.g. wetlands, (Tjerngren et al., 2012a; b), lake sediments (Bravo et al., 2017), stratified water columns (Eckley et al., 2005) and even in micro-environments of settling particles (Gascón Díez et al., 2016). The formation of MeHg is ascribed to the activity of anaerobic microorganisms (e.g., iron- or sulfate-reducing bacteria, archaea) (Zhang et al., 2012, 2014; Hammerschmidt and Fitzgerald, 2004; Tjerngren et al., 2012a; b; Parks et al., 2013). Indeed, Hg(II) methylation processes are governed by the activity of the microbial community (Bravo et al., 2017), as well as the availability of Hg(II) to methylating microorganisms, which in turn is dependent on the Hg(II) speciation (Gerbig et al., 2011, 2012; Jonsson et al., 2012, 2014; Zhang et al., 2012, 2014). The Hg mobilization, speciation, and methylation have been widely studied across various environments (Skyllberg, 2008, 2012; Graham et al., 2012, 2013).

Of all the biogeochemical variables affecting Hg transformations, DOM is one of the most important factors (Aiken et al., 2011a; Ravichandran, 2004; Gerbig et al., 2012; Bravo et al., 2017; Herrero Ortega et al., 2017). There are many reports on the interactions and correlations between DOM and Hg, and comprehensive reviews are available elsewhere (Ravichandran, 2004; Aiken et al., 2011a; b; Skyllberg, 2012; Gerbig et al., 2012; Hsu-Kim et al., 2013). In field investigations, correlations between concentrations of DOC and Hg have been established to indicate the role of DOM (Mierle and Ingram, 1991; Driscoll et al., 1995; Hurley et al., 1998; Dittman et al., 2009; Bergamaschi et al., 2012). However, across aquatic systems, influenced by diverse biogeochemical processes and sources of DOM, the correlation between concentrations of Hg and DOC is not always consistent. Lab-scale experiments have revealed a dual effect of DOM on MeHg net production, by i) acting as a stimulatory electron donor, and by ii) modulating the chemical speciation of Hg(II). DOM also serve as a substrate for microorganisms and stimulate Hg methylation (Hsu-Kim et al., 2013; Schartup et al., 2013; Gerbig et al., 2012; Kim et al., 2011). Indeed, most groups of microbes containing phyla of Hg methylators are key anaerobic decomposers of organic materials (Gilmour et al., 2013; Reddy and Delaune, 2008; Logue et al., 2016). Under sulfidic conditions, a stimulatory effect of DOM on MeHg production is attributed to the disintegration or dissolution of HgS-minerals (Waples et al., 2005), resulting in enhanced Hg(II) bioavailability to methylating bacteria (Gerbig et al., 2011; Graham et al., 2012, 2013). In contrast, chemisorption to DOM functional groups may limit Hg(II) bioavailability for methylating microorganisms when the molecular size of DOM is too large to cross the bacterial cell membranes (Hammerschmidt and Fitzgerald, 2004; Hammerschmidt et al., 2008). Recent studies (Schartup et al., 2013; Chiasson-Gould et al., 2014; Bravo et al., 2017; Herrero Ortega et al., 2017; Lescord et al., 2018; Noh et al., 2018) demonstrate that differences in the composition of DOM may largely explain the variability in Hg methylation. Indeed, it is known that specific DOM components regulate speciation and dynamics of Hg through numerous mechanisms, including chemical complex formation (Ravichandran, 2004; Skyllberg, 2008, 2012), redox processes (Gu et al., 2010) and microbial activity (Bravo et al., 2017). Thus, all the mentioned studies underscore the complexity of the interactions between Hg and DOM, and more importantly, highlight the potential to perform comprehensive studies to identify the Hg risk, especially the MeHg net production in the environment using DOM composition.

Despite the recently highlighted importance of DOM composition and quantity, environmental biogeochemical studies of Hg still poorly or incompletely take DOM characterization into account, especially outside the boreal zone. Here we use the variability in DOM characteristics to improve our understanding about how concentrations of DOM and Hg may be related (or not related) at different study sites in subtropical China. We hypothesize that, beyond DOC concentration, DOM composition characteristic of terrigenous and aquatic sources are important drivers behind Hg concentration levels and the transformation of Hg to MeHg in different types of lakes located at southern latitudes. Based on the "structure-reactivity" concept of DOM biogeochemistry (Senesi et al., 2009; Aiken et al., 2011a; b), we: 1) characterized the properties of porewater DOM in three lakes of southwest China, and 2) tracked DOM sources to elucidate their influence on Hg concentration levels and transformation to MeHg in lake porewaters. Our results demonstrate optical characterization of DOM as a useful tool to improve our understanding of the causality behind DOM-Hg relationships established by field observations of three different lakes.

2. Materials and methods

2.1. Study sites

On the Southwestern China Plateau, there are more than 30 lakes with a water depth of 10–50 m. Three of these lakes, Caohai Lake (CH), Hongfeng Lake (HF) and Wujiangdu Lake (WJD), were selected for this study (Fig. 1). Caohai Lake (CH) (26°50′50″N, 104°14′27″E) is in southwestern Weining County of the Guizhou Province. It is a pristine shallow lake located in the Caohai State Nature Reserve. The catchment of CH includes evergreen broad-leaf forests with riparian soils exporting terrestrial DOM into CH, especially during high precipitation periods between May and October (Qian et al., 2008). Established in the 1960s, Hongfeng Lake (HF) (26°33′05″N, 106°25′25″E) is in the suburbs of Guiyang City, Guizhou province, China. It is one of the main municipal drinking-

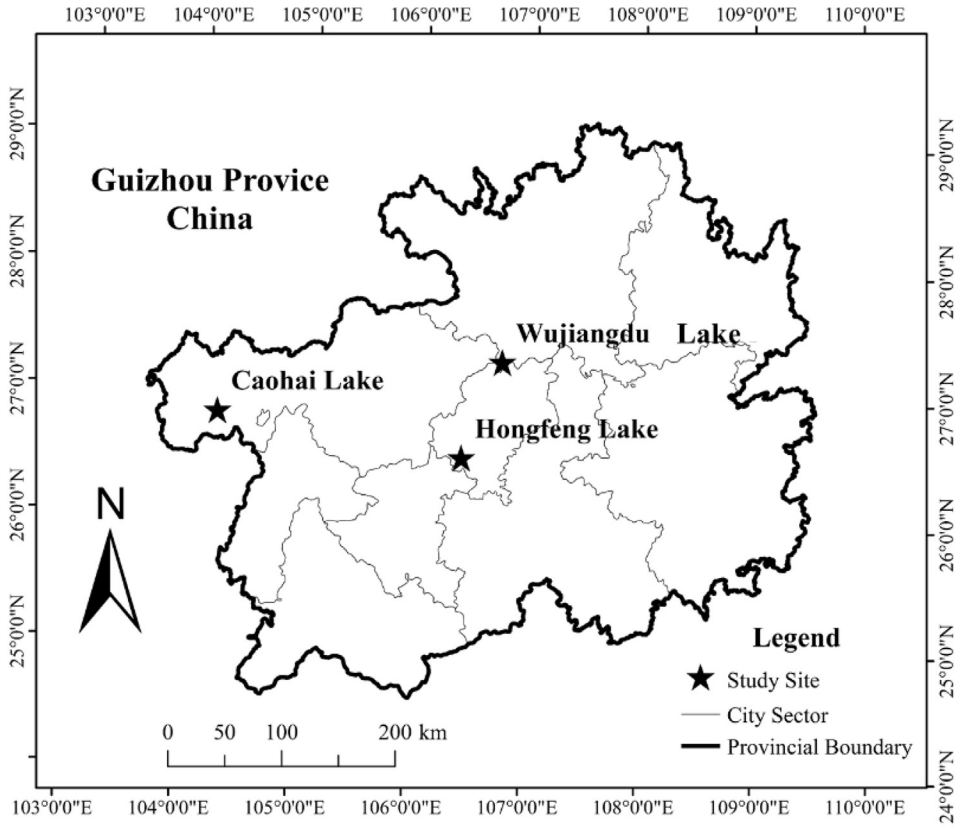

Fig. 1. Study area and the locations of Caohai Lake (CH), Hongfeng Lake (HF) and Wujiangdu Lake (WJD) in Guizhou province of China.

water reservoirs. It is a lake with seasonally anoxic bottom waters, having an average water depth of 10.5 m. Wujiangdu reservoir (WJD) (27°19′11″N, 106°45′40″E) is situated on the Wujiang River, which is a branch of Yangtze River, Guizhou Province. This reservoir was formed in 1979. Both HF and WJD are impacted by anthropogenic activities (e.g., urban development, cage aquaculture), in contrast to CH which is a natural lake. Additionally, unlike WJD, HF lake is influenced by terrestrial DOM inputs from adjacent dryland runoff to a certain degree. More details are in Supporting Information (Table S1).

2.2. Sample collection, DOM and Hg analysis

In July 2014, sediment cores were collected in the middle of the three lakes (Fig. 1) using a sediment gravity corer. Nine cores were sampled at 0–9 cm depth at CH and WJD and seven cores at HF. Water quality parameters were measured *in situ* with a portable multi-parameter water quality probe. Sediment cores were processed within a few hours at the sampling site in oxygen-free glove bags filled with nitrogen gas in the laboratory following centrifugation (2000 g for 30 min), the pore water was filtered using 0.45 μm Millipore PVDF filters in the glove bag and the supernatant was divided for analysis of pore water Hg and DOM in an anoxic atmosphere. Samples for dissolved Hg measurements were acidified by adding 0.5% (v/v) ultrapure HCl. All the liquid samples were preserved at 0–4 °C prior to analysis and the solid sediment was stored in a freezer prior to Hg analysis.

The DOM concentration was measured using a TOC analyzer (GE Sievers InnovOx, USA), represented as dissolved organic carbon (DOC) in mg L^{-1}. The hydrophobic carbon fraction of DOM (HDOC) was separated from hydrophilic fractions by an XAD-8 resin (Supporting Information 2) and is expressed as DOC in mg L^{-1}. Additionally, we measured total nitrogen (TN), nitrate (NO_3^-) and ammonium (NH_4^+) to calculate the total dissolved organic nitrogen (DON) by subtracting NO_3^- and NH_4^+ from TN in the DOM sample. The N/C molar ratio was calculated by DON/DOC. TN analysis was conducted by the potassium persulfate oxidation-UV colorimetric method. Nitrate and ammonium were measured by ion-selective electrodes (Bante Instrument Shanghai, China). UV–Vis and fluorescence measurements were conducted in a 10 mm quartz cuvette using Aqualog® (Horiba, Japan) absorption-fluorescence spectroscopy equipped with a 150 W ozone-free xenon lamp at constant 20 °C temperature. Milli-Q water was used as blank to be subtracted from sample EEMs to remove the interferences of water Raman peaks. Using the parallel absorbance measurement from the same sample and blank (Yang and Hur, 2014), EEMs were corrected for inner-filter effect by Aqualog® EEMs data processing software automatically, which also adjusted the instrument specific excitation and emission effects. These corrections were also manually double-checked in OriginPro® 2015. The UV–Vis scan ranged from 230 to 800 nm with 1 nm interval. The Naperian absorption coefficient was calculated as $a(\lambda) = 2.303^*A/l$, where $a(\lambda)$ is the DOM absorption coefficients at wavelength λ (nm), A is the absorbance, and l is the cuvette path length (m) (Coble, 2007; Helms et al., 2008). The absorption coefficient at 355 nm (a_{355}) was chosen to represent the quantity of chromophoric DOM (CDOM) (Rochelle-Newall and Fisher, 2002; Zhang et al., 2005). Because of the pore-water DOM samples is highly concentrated in DOC, the diluted (DOC<10 mg L^{-1}) samples were used for all spectra (including absorption and fluorescence) to avoid inner-filtration effects. The original CDOM (i.e., a_{355}) (m^{-1}) reported in this study was calculated by the measured values multiplied by the dilution factor.

Additionally, EEMs fluorescence spectra were collected. The emission spectral range was 250–620 nm in 3.18 nm steps and the excitation spectral range was 230–450 nm in steps of 5 nm. The scan integration time was 3s.

Porewater concentrations of dissolved Hg and MeHg were determined at the Institute of Geochemistry of CAS, Guiyang. Two dissolved Hg species including total Hg (DTHg) and MeHg (DMeHg) in 0.45 μm filtered water samples were measured in this study. In this paper, DTHg and DMeHg represent the dissolved species of Hg, unless otherwise specified. They were determined based on the strict procedure of pre-cleaning, purging, trapping and cold vapor atomic fluorescence spectroscopy (CVAFS). Concentrations of THg in porewater were measured using dual stage gold amalgamation and cold vapor atomic fluorescence spectrometry (CVAFS, Tekran®, model 2500, Canada), following sample pre-oxidation by 0.5% v/v BrCl, reduction by 0.2% v/v $NH_2OH{\cdot}HCl$ and $SnCl_2$, and pre-concentration of Hg^0 onto a gold trap with an aspirator. MeHg was measured using GC-CVAFS (Model III, Brooksrand®, USA) after distillation and ethylation following EPA method 1630. To help explain dissolved Hg in porewater, total Hg and total MeHg in sediment were also measured by thermal combustion method (AMA 254, Leco®, USA) and HNO_3 leaching/CH_2Cl_2 extraction-ethylation-GC-CVAFS detection (Tekran® model 2500, Canada), respectively. For QA/QC, methods were conducted with field blanks, method blanks, matrix spikes, duplicate samples, and statistical analysis of the resulting analytical data. For water samples, the detection limits obtained from the method blanks (blank ± 3 standard deviations) for THg and MeHg were 0.09 and 0.03 ng L^{-1}, respectively. Additionally, recovery was controlled with matrix spikes because the MeHg measurements required an extraction procedure. The MeHg spike recovery was in the range of 85.4–98.2%. The detailed descriptions of sample collection, preparation and measurement are referred to in Yan et al. (2013) and Zhao et al. (2017).

2.3. DOM spectral parameters

Specific UV absorbance at 254 nm ($SUVA_{254}$), associated with DOM aromaticity and humification, was calculated as A_{254} normalized for DOC concentration and corrected for Fe (Weishaar et al., 2003). In both the wavelength ranges of 275–295 nm and 350–400 nm, the spectral slope of DOM absorption curve was fitted by nonlinear regression by the function: $a(\lambda) = a(\lambda_r)^*\exp[-S(\lambda-\lambda_r)]$, where λ_r is a reference wavelength. However, $S_{275\text{-}295}$ and $S_{350\text{-}400}$ showed little compositional variations in our DOM samples. Importantly, previous studies demonstrated S_R to be a more appropriate characteristic of DOM in samples sets with a large variability in chemical properties (Helms et al., 2008; Spencer et al., 2012). Thus, we calculated the spectral slope ratio by $S_R = S_{275\text{-}295}/S_{350\text{-}400}$ (Helms et al., 2008). Additionally, parallel factor analysis (PARAFAC) was not included in this study because the limited number of samples originating from quite diverse sources. Instead, a classic "peak-pick" method was used to identify the fluorescent peaks (Coble, 1996, 2007; Coble et al., 2014). We identified four fluorescent components including: (1) two humic-like components represented by A (E_x/E_m = 250–260nm/380-480 nm), C (E_x/E_m = 330–350nm/420-480 nm), and (2) two protein-like component tryptophan-like T (E_x/E_m = 270–280nm/320-350 nm) and tyrosine-like peak B (E_x/E_m = 270–280nm/300-320 nm). For distinguishing DOM sources, fluorescence index (FI) was calculated as the ratio of the fluorescence intensities at the emission wavelength of 450 and 500 nm (excitation wavelength was kept at 370 nm) (McKnight et al., 2001; Huguet et al., 2009). Additionally, as an indicator for reflecting the recent microbial-production of DOM (i.e., autochthonous inputs), BIX, also called freshness index, was calculated using the ratio of emission intensity at 380 nm divided by the emission intensity of the maximum value in the range of 420–435 nm at the excitation of 310 nm (Wilson and Xenopoulos, 2009; Fellman et al., 2010).

2.4. Two end-member mixing model of DOM

We used the nitrogen/carbon (N/C) molar ratio to estimate the fractions of allochthonous and autochthonous contributions to DOM (Perdue and Koprivnjak, 2007) based on two-member mixing. We used equation (1) to calculate the contribution of the two fractions:

$$\frac{N}{C} = f_{auto} \times \left(\frac{N}{C}\right)_{auto} + f_{allo} \times \left(\frac{N}{C}\right)_{allo} \quad (1)$$

where f_{auto} and f_{allo} represent organic matter from autochthonous and allochthonous origins, respectively. The ratios $(N/C)_{auto}$ and $(N/C)_{allo}$ are typical values of the two end-member, gathered from the literature. Eq. (1) can further be arranged to Eqs. (2) and (3):

$$f_{auto} = \frac{\left(\frac{N}{C}\right)_{allo} - \left(\frac{N}{C}\right)}{\left(\frac{N}{C}\right)_{allo} - \left(\frac{N}{C}\right)_{auto}} \quad (2)$$

$$f_{allo} = \frac{\left(\frac{N}{C}\right) - \left(\frac{N}{C}\right)_{auto}}{\left(\frac{N}{C}\right)_{allo} - \left(\frac{N}{C}\right)_{auto}} \quad (3)$$

2.5. DOM biodegradation test

Indigenous population of microbial communities in the sediment was used in the method, following the literature (Peretyazhko and Sposito, 2006; Kappler et al., 2004). No further microbial identifications were done. Sediments were weighed and mixed with DI water to form aqueous sediment suspensions (15 mg L^{-1}) with 10 mM sodium acetate added as an electron donor. Suspensions were horizontally oscillated (200 rpm) at 25 °C in the anoxic glovebox for 72 h. After which, they were filtered through 0.22 μm Millipore filters to retain the microorganisms. Filters were rinsed with a 50 ml bicarbonate buffer (pH = 7.0) and collected. After that, sterile-filtered (0.22 μm Millipore filters) IHSS standard DOM samples (IHSS 1R105F Nordic Reservoir fulvic acid sample, 30 mg.L^{-1}) were inoculated with the indigenous microbial community solution in 100 ml blue-cap bottles with 25 ml headspace with N_2 (99.99%). During the 16-day batch incubations, the DOM samples were collected at time intervals of 3, 6, 10 and 16 days, respectively, for DOC measurement.

2.6. Statistical analyses

All results were reported as mean values of, at minimum, duplicates and statistical analyses were done in OriginPro® 2015 and SPSS® 24. All data were tested for normality by the Lilliefors test (Supporting Information 3). Pearson correlation (r) and Spearman's rank correlation (r_s) were conducted on normally or non-normally distributed data, respectively. Additionally, analysis of variance (ANOVA) and Kruskal-Wallis test were conducted to test the differences for normal or non-normal distributed data-set, respectively, by SPSS® Statistics 24. Statistical significances were defined at $p < 0.05$ and $p < 0.01$ indicating "significant" and "highly significant" differences, respectively. The actual p values are given in the text with three decimals.

3. Results and discussion

3.1. DOC and CDOM

The porewater DOC concentration ranged from 30.3 to 90.4 mg. L^{-1} (Supporting Information 4, Table S3). By the one-way ANOVA, the difference in DOC concentration between CH and the other two lakes was significant ($p = 0.031$), but no significant difference was observed between HF and WJD. The lowest DOC concentration was observed in CH (Fig. 2-a). The CDOM/DOC ratio was calculated to estimate the relative contribution of CDOM to the bulk DOC. In the three lakes, the average CDOM/DOC (L mg-C^{-1} m^{-1}) was 0.34 (CH), 0.27 (HF) and 0.30 (WJD) (Fig. 2-a), respectively, showing the relative contribution of CDOM was greater in CH. The CDOM has been used as a proxy to predict the DOC by linear regression (Spencer et al., 2012; Asmala et al., 2012; Jiang et al., 2017a). The linear regressions between CDOM and DOC is improved when the light-absorption components of DOM are more predominant. (Fig. 2-b). The weaker relationship between CDOM and DOC in HF and WJD, may indicate a higher contribution from non-chromophoric DOM in this lake, which is known to have a larger urban (human) influence.

3.2. UV–Vis absorption spectral characteristic

The average $SUVA_{254}$ in the CH lake (3.9 L mg C^{-1} m^{-1}) was significantly higher than in other two lakes (average 2.8 for HF; 3.2 for WJD) ($p = 0.035$), indicating the highest aromaticity of DOM was in CH. Hydrophobic carbon covaried with $SUVA_{254}$ (Fig. 3-a). When normalized to DOC, the percentage of HDOC and %(HDOC/DOC) was highest in lake CH (Fig. 3-b), having approximately 50% of DOC in the form of hydrophobic carbon. Although DOC concentrations were higher in HF and WJD, the contributions of non-aromatic (i.e., low hydrophobic) moieties (e.g., sugar and protein) were important as indicated by the lower %HDOC.

The spectral slope ratio (S_R=$S_{275\text{-}295}$/$S_{350\text{-}400}$) (Helms et al., 2008) ranged from 0.79 to 1.89 (Fig. 3-c), was higher than the values reported for a bog and fen (Tfaily et al., 2013) but similar to marshes (Clark et al., 2014), streams/rivers (He et al., 2016) and coastal sediments (Dang et al., 2014) with anthropogenic influences. The S_R seems to correlate negatively with DOM molecular weight (Fichot and Benner, 2012; Fichot et al., 2013). In this study, the lowest S_R values (range of 0.79–1.18) were observed in CH. In CH, S_R also showed a significant, negative correlation with $SUVA_{254}$ (Fig. 3-c), indicating that aromatic components contribute to the DOM molecular weight in this pristine natural lake. Higher S_R values and lower $SUVA_{254}$ in HF and WJD lakes, as compared to CH, indicate an enrichment in low molecular weight compounds (e.g. some proteins or polysaccharide) and less aromaticity. This may suggest an important contribution from microbial/algal sources to the DOM signature in the sediments at HF and WJD, which was validated by further fluorescence spectral analysis and the biodegradation assay reported below. Additionally, the significantly inverse correlation between DOC and $SUVA_{254}$ ($r = -0.89$, $p = 0.001$) was only observed in WJD, further supporting this explanation and indicating the importance of the autochthonous contribution for DOC increases (Kothawala et al., 2014; Jiang et al., 2018a; b).

3.3. Fluorescence spectral characteristic

Examples of the DOM EEMs spectra of the collected porewater are shown in Fig. 4. Protein-like components, Peak B and T, are readily linked to DOM lability (Fellman et al., 2009), anthropogenic interferences (Baker, 2001, 2002) and microbial activities (Fasching et al., 2014). After normalization by DOC, to remove the concentration-dependence, the lower peak B/DOC and peak T/DOC in CH suggest relatively less microbial material contribution to the DOM composition. Recently, some researchers proposed using Peak T alone to assess the water quality, because of its significant correlation with microbial activities (e.g., microbial number) (Baker et al., 2015; Sorensen et al., 2018a; b; Nowicki et al., 2019). A higher protein peak signatures, especially the Peak T, observed in samples of HF and WJD, may therefore may indicate a larger contribution from microbial-derived DOM driven by greater microbial activities than suggested by the optical signature in the porewater of CH.

Both HF and WJD lakes were formed artificially to establish hydroelectric power generation and have a different degree of eutrophication caused by the accumulation of nutrients (Shang et al., 2011; Zhao et al., 2017), which induce the proliferation of algae and phytoplankton (Shang et al., 2011; Zhao et al., 2017) that also could heavily influence the abundance of protein-like components in the DOM (Zhou et al., 2015, 2017). Local long-term cage aquaculture activities are also key factors for the high protein-like signatures caused by the high primary production at the two sites (He et al., 2010; Feng et al., 2012). Thus, DOM optical signatures of HF and WJD indicate important contributions from anthropogenic effluences, active microbial metabolism and algae/phytoplankton blooms.

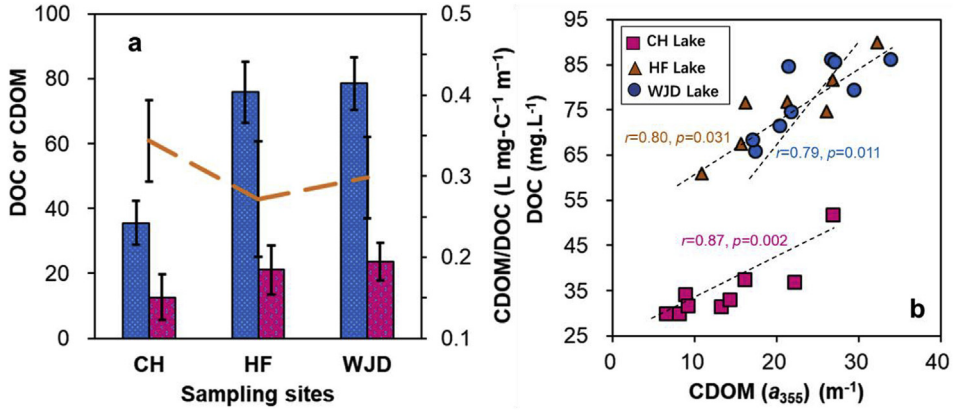

Fig. 2. (a) Quantities of DOC (mg. L^{-1}) and CDOM (m^{-1}), and the CDOM/DOC ratio (L mg-C^{-1} m^{-1}); (b) Relationship between DOC and CDOM in samples from the three lake sediments. In plot (a), the left y-axis represent DOC (blue-small dot bar) and CDOM (purple-medium dot bar) levels. The organe dash line is CDOM/DOC ratio. (For interpretation of the references to color in this figure legend, the reader is referred to the Web version of this article.)

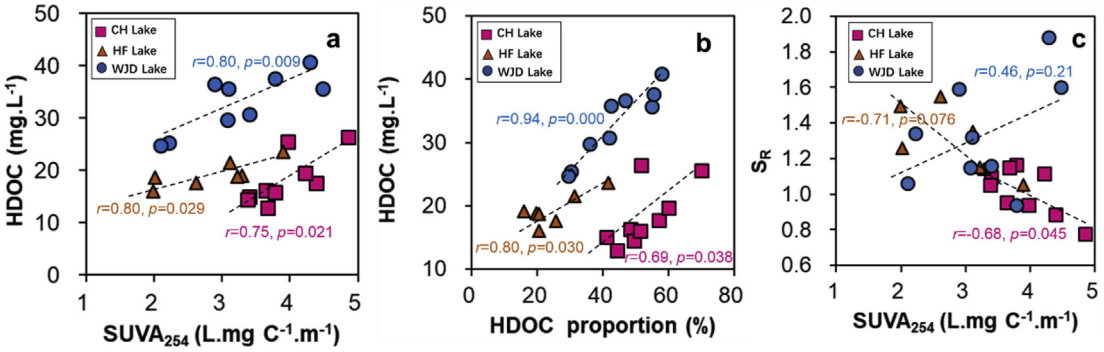

Fig. 3. Correlation between $SUVA_{254}$ and (a) hydrophobic carbon (HDOC), (b) HODC and HDOC proportions, and (c) S_R in porewater samples from the three lake sediments. Only significant relationships are shown. In WJD, no significant correlation between $SUVA_{254}$ and S_R was observed ($p > 0.05$).

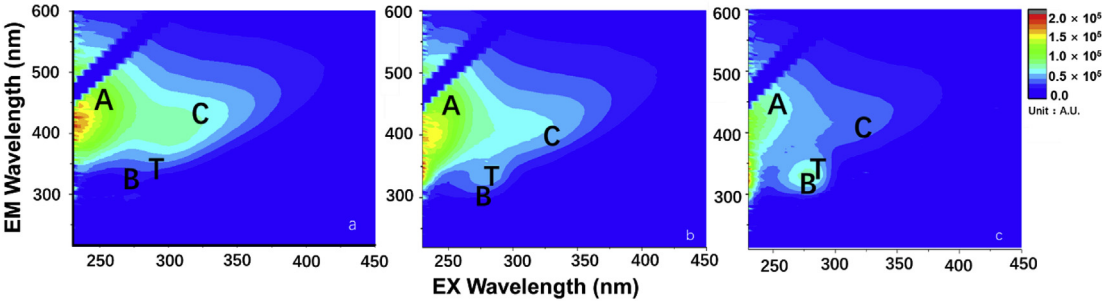

Fig. 4. Typical excitation-emission matrices (EEMs) of sediment porewater DOM collected from the three lakes CH (a), HF (b) and WJD (c). Fluorescence intensities (z-axis) have in arbitrary units (A.U). Peaks A and C are humic-like fluorescence components (proxies for relatively recalcitrant DOM, assumed to be allochthonous) and peaks B and T are protein-like fluorescence components (proxies for labile DOM, assumed to be autochthonous).

3.4. Fluorescence indices and two end-member mixing model of DOM

Fluorescence indices (e.g., FI, BIX and *r*(T/C)) are useful tools to characterize DOM. There are several studies in which these indices has been used and interpreted in pristine and anthropogenically impacted surface waters (McKnight et al., 2001; Baker, 2001, 2002; Huguet et al., 2009; Kothawala et al., 2012; Gabor et al., 2014). Furthermore, they are extensively used to characterize DOM from other sources, such as organic aerosols (Fu et al., 2015), fogwater (Birdwell and Valsaraj, 2010), cave and spring water (Birdwell and Engel, 2010) and sediment porewater (Burdige et al., 2004; He et al., 2016; Guillemette et al., 2017).

Autochthonous (i.e., microbial/algae) and allochthonous (i.e., terrestrial) sources can be identified by a FI higher than 1.9 or lower than 1.4, respectively (McKnight et al., 2001; Huguet et al., 2009). Accordingly, while CH had FI values lower than 1.4, suggesting a predominant allochthonous source, FI values for HF and WJD indicated a combination of autochthonous and allochthonous sources, with WJD more influenced by autochthonous (i.e., microbial/algal/anthropogenic effluent) sources than by allochthonous (i.e., terrestrial) sources (Fig. 5-a). The BIX at HF and WJD was both exceeding 0.8, and in particular WJD had significantly higher values than CH and HF. This is good agreement with the results at FI, confirming the contribution of biologically-derived autochthonous DOM in lake WJD (Fig. 5-a).

Two intensity ratios of fluorescent peaks, *r*(A/C) and *r*(T/C), were calculated (Fig. 5-b). The *r*(A/C) peak is used to reflect the relative proportion of the two humic-like components in DOM and to distinguish relatively "less processed" humic material from the more "processed" pool. One rationale for this is the observed increase in the *r*(A/C) ratio due to a preferential loss of peak C in relation to peak A in photo- or bio-degradation processes (Kothawala et al., 2012). Lower average *r*(A/C) value in CH (2.76) as compared to 3.37 in HF and 6.47 in WJD indicates a possible enrichment of non-processed humic substances in CH. As an important indicator of water quality, *r*(T/C) is also used to track influences of wastewater and anthropogenic interferences (Baker, 2001, 2002; Galapate et al., 1998). This empirically, *r*(T/C) higher than approximately 2.0 indicates significant influence of anthropogenic effluences (Baker, 2001, 2002; Old et al., 2012; Carstea et al., 2016). In HF and WJD most DOM samples showed *r*(T/C) higher than 2.0. Also, *r*(T/C) was significantly higher in HF and WJD than in CH ($p = 0.016$), but without significant difference between them ($p = 0.21$). This higher microbial activity indicated by *r*(T/C) in HF and WJD also agrees with the peak T observed as abovementioned.

As shown in Fig. 6, the contributions from allochthonous DOM sources, as calculated by the two-member mixing model, were largest in lake CH porewater and lowest in WJD. Based on previous studies of typical algae/bacterial and terrestrial/humic OM sources, we used typical N/C molar ratios values of 0.1 and 0.02 for autochthonous and allochthonous DOM, respectively (Perdue and Koprivnjak, 2007). The mixture of allochthonous and autochthonous sources of DOM showed a great consistency among the 7–9 sediment samples within each lake (Fig. 6). The trend among the three lakes was that the CH lake had the highest terrestrial source contribution (66–83%), followed by HF (40–75%) and the WJD lake had the smallest contribution from terrestrial/humic sources (11–45%). This trend is well in agreement with the reported $SUVA_{254}$ and FI values and relationships of each of those with DOM in the three lakes (Figs. 3 and 5). Thus, these mixing model results in further agreement with the spectral results, that the different characteristics of DOM are heavily dependent on the sources and anthropogenic activity.

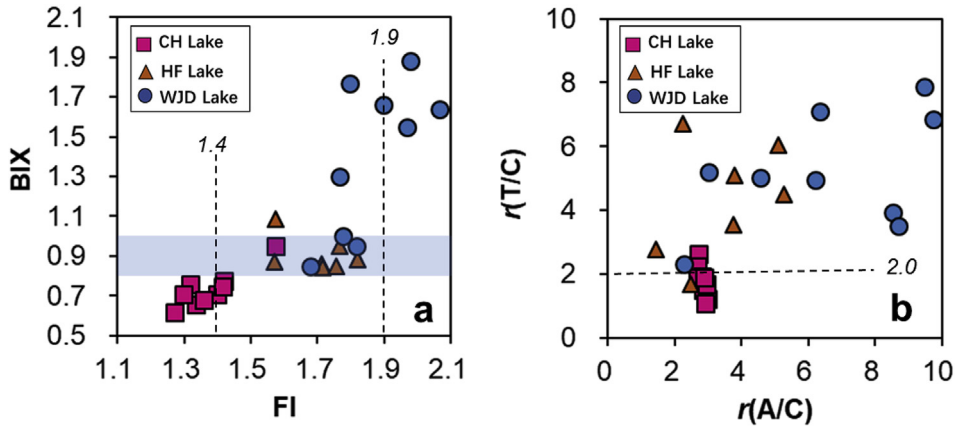

Fig. 5. Comparison plots of FI versus BIX (a), and *r*(A/C) versus *r*(T/C) (b) for porewater DOM from the three lake sediments. In plot (a), the light blue shadow region indicates significant autochthonous origins, areas above it reflects predominant biological (i.e. microbial/algae) origins, as outlined by (Huguet et al., 2009). Additionally, the region to the left of the dashed line at FI = 1.4 indicates terrestrial-dominated CDOM; the region to the right of the dashed line at FI = 1.9 indicates microbially-dominated CDOM (McKnight et al., 2001); and the region between the two dashed lines represents mixed signatures. In plot (b), *r*(T/C) > 2.0 indicates an obvious influence of anthropogenic effluences. (For interpretation of the references to color in this figure legend, the reader is referred to the Web version of this article.)

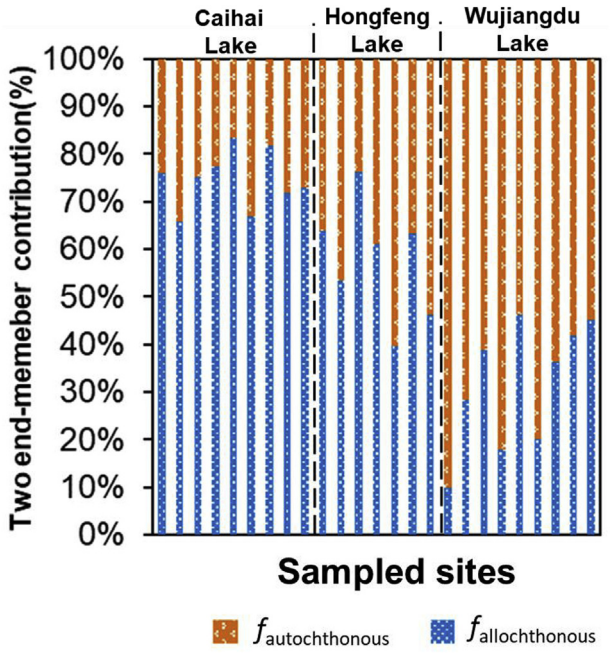

Fig. 6. Two end-member contributions from allochthonous and autochthonous OM sources to sediment porewater DOM from the three lake sediments. From left to right follows 9 sediment cores from Caihai Lake (CH Lake), 7 sediment cores from Hongfeng Lake (HF Lake) and 9 sediment cores from Wujiangdu lake (WJD Lake). Blue (f_{allo}) represents allochthonous red (f_{auto}) represents autochthonous OM contribution. (For interpretation of the references to color in this figure legend, the reader is referred to the Web version of this article.)

In conclusion, our results show strong signs that DOM in the sediment porewaters of all three lakes is a mixture of allochthonous and autochthonous sources. Porewater in CH lake sediment is clearly controlled by terrestrial inputs, showing a distinctly higher humic character as compared to the other two lakes. In contrast, samples from HF and WJD were more inclined to be influenced by autochthonous algal/bacterial organic matter production.

3.5. Concentrations of mercury in porewater and sediment

Concentrations of DTHg and DMeHg ranged over more than one order of magnitude (1.8–17.3 and 0.002–9.4 ng. L^{-1}, respectively). Lake HF and WJD showed higher concentrations of DTHg ($p = 0.026$) than CH lake (mean 3.1 ng. L^{-1}), but the highest DMeHg concentration was found in WJD (mean 2.1 ng.L^{-1}) (Fig. 7-a). A significant relationship between DMeHg and DTHg (Fig. 7-a) ($p = 0.013$) was only observed in lake WJD. To resolve the underlying processes behind relationships between total Hg and MeHg concentrations in sediment and porewater we need to consider several factors and processes (Skyllberg, 2008; Drott et al., 2008; Jonsson et al., 2012, 2014). The porewater Hg concentration is controlled by two factors: (1) inorganic Hg storage, and (2) the partition of Hg between aqueous and solid phases. The concentration of MeHg in porewater is similarly dependent on the total concentration of MeHg in the sediment and its partitioning into the aqueous phase but is also affected by the rate of MeHg net formation by methylating bacteria and subsequent demethylation. The bacteria in turn require electron-donors (labile OM), electron-acceptors (e.g. H_2, sulfate, Fe(III)) and inorganic Hg, which serves as a substrate for the MeHg formations. Based on this thinking, the ratio of MeHg/THg (%MeHg) in sediment (Skyllberg, 2008; Drott et al., 2008) has been shown to be a relevant proxy for the net Hg methylation efficiency at a specific site. Like the analysis of porewaters, WJD showed the highest %MeHg and absolute MeHg concentration in sediments (Fig. 7-b, and Fig. S1), indicating the greatest methylation potential of the three lakes.

The average distribution (partition) coefficient (K_d, L.kg^{-1}), calculated as $K_d = C_s/C_w$, where C_s (mg.kg^{-1}) and C_w (mg. L^{-1}) are the concentrations in the solid and aqueous phases, respectively, did not show any significant differences among the three lake sediments (Fig. 7-b-b). Thus, the partition of THg, commonly caused by differences in solid phase composition of Hg or in concentrations of high-affinity ligands (thiols and inorganic sulfides) did not differ among the three lakes. The concentration of MeHg, both in sediment and porewater, differed substantially among the three lakes (Figs. S1–a), being most concentrated in WJD lake sediments and least concentrated in CH.

3.6. Environmental implication of porewater DOM properties: associations with Hg

A strong positive correlation between Hg and DOC concentration is often reported in studies of boreal and temperate forest

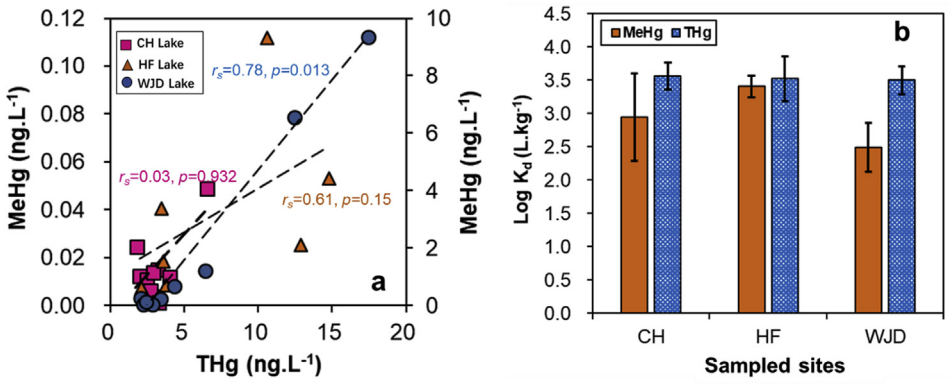

Fig. 7. Mercury concentrations in the porewater and sediment showing (a) the relationship between dissolved MeHg and dissolved THg in sediment porewaters of the three lakes, with data from WJD lake plotted on the right y-axis, and (b) the distribution (partition) coefficient (K_d, L.kg^{-1}) for THg and MeHg, calculated as $K_d = C_s/C_w$, where C_s (mg.kg^{-1}) and C_w (mg.L^{-1}) are the Hg or MeHg concentrations in the solid and aqueous phases, respectively. For convenience, K_d is often logarithmically expressed as log K_d. Error bars represent ±SD.

streams, suggesting that Hg fate in aquatic systems is linked with DOM (Mierle and Ingram, 1991; Driscoll et al., 1995; Hurley et al., 1998; Dittman et al., 2009; Bergamaschi et al., 2012). In this study (Supporting Information 6, Fig. S2), only CH lake showed a significant, positive correlation between DOC and DTHg ($p = 0.033$). The fact that DTHg was positively correlated also with $SUVA_{254}$ (Fig. 8-a), BIX (Figs. S3–a) and FI (Figs. S3–b) (Supporting Information 7, Fig. S3), indicates that DOM was enriched in terrestrial DOM and points at terrestrial inputs being the major source of Hg in lake CH. Terrestrial inputs has been highlighted as important sources of THg for streams (Eklöf et al., 2012; Bravo et al., 2018). In comparison to the other two lakes, the lack of correlation between DTHg and protein parameters (e.g., peak T and r(T/C)) is consistent with CH being a natural pristine lake highly influenced by terrestrial soil runoff. The negative relationship between DTHg and S_R (Figs. S3–c) further supports the notion that DTHg variability is heavily dependent on DOM molecular mass distribution. Yet, significant correlations between DMeHg and BIX (Fig. 8-b) and FI (Figs. S3–d) suggest that MeHg levels in porewater were associated with microbial activities in lake CH. This is supported by the negative relationship found between of dissolved DMeHg and S_R (Figs. S3–e) which indicates high DMeHg concentrations linked to the presence of low molecular mass DOM. Microbial DOM processing could result in high optical signatures of low molecular mass protein-like components (Helms et al., 2008) and enhance Hg(II) methylation (Bravo et al., 2017; Noh et al., 2018; Herrero Ortega et al., 2017).

Lake HF presented a contrasting DOM signature compared to CH. For example, DTHg and DMeHg did not show any significant correlation with neither DOC nor CDOM (Fig. S2). In this lake, autochthonous DOM seemed to be a predominant factor responsible for Hg variability in porewater, as indicated by the significant negative correlation of DTHg ($p = 0.003$) and DMeHg ($p = 0.030$) with FI (Fig. 8 c and d). Additionally, the correlation between DMeHg and BIX (Supporting Information 8, Fig. S4-a), and between MeHg and protein-like peak T (Figs. S4–b) reveals a link between microbial activities and MeHg concentration. Yet, DMeHg was negatively correlated to r(T/C) (Figs. S4–c) in HF, possibly indicative

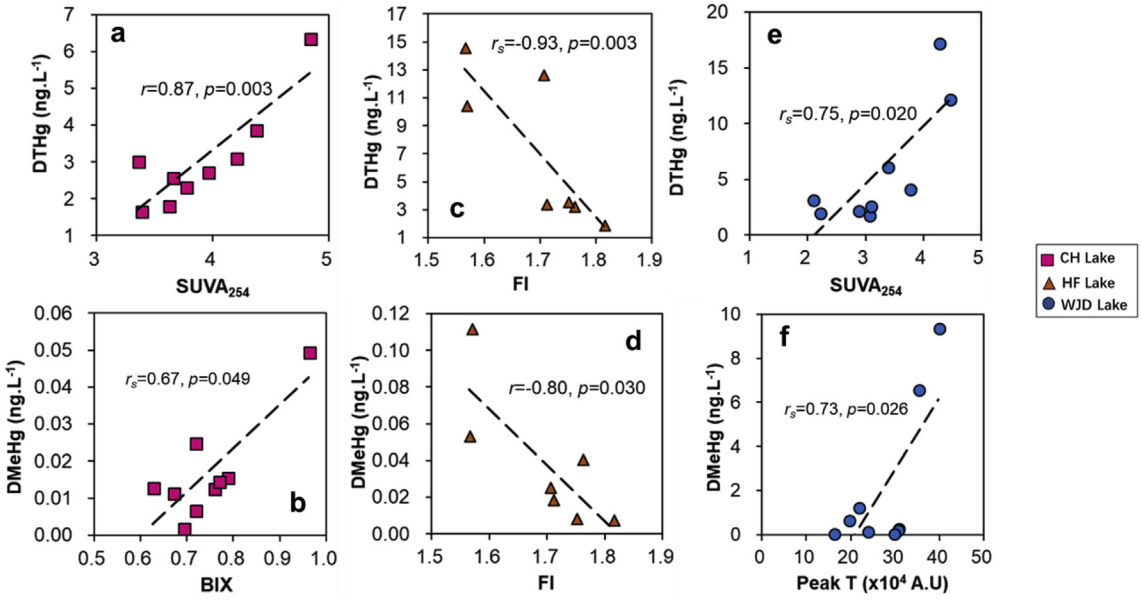

Fig. 8. Typical correlations between dissolved Hg species and the relevant DOM optical parameters in the three lake sediment porewaters.

of an inhibitory effect on MeHg net production caused by a change from more humic-like to protein-like components. Yet, as aforementioned, protein-like components in porewater DOM in lake HF may not originate only from autochthonous production but also from anthropogenic effluents (Fig. 5-b). Thus, this negative correlation may be the effect of the dilution of protein-like characteristics by elevated anthropogenic wastewater inputs, instead of merely a consequence of microbial/algae production. A similar "dilution effect" may also explain the negative correlation between DTHg and FI (Fig. 8-c), and between DMeHg and FI (Fig. 8-d). Other possible reason may be that the Hg associated with autochthonous DOM could deposit in sediments of relative stagnant water bodies such as lake HF. This explanation is also supported by the large K_d value (Fig. 7-b), indicating that solid phase partitioning was an important factor behind the relationship between Hg and DOM in lake HF porewater.

In WJD, DTHg was inversely correlated with DOC (Supporting Information 9, Figs. S5–a) and BIX (Figs. S5–b), suggesting that high DOC concentrations with microbial/algae signatures could be associated with a decrease in DTHg. These relations could be explained by two processes: (1) biodilution (Pickhardt et al., 2002) and/or, (2) abiotic reduction of Hg(II) by DOM. The first process is enhanced by bacterial uptake and/or adsorption of Hg onto biomass surfaces during high algal and bacterial production, which results in high DOC concentrations and BIX values. The latter process, abiotic reduction of Hg(II) by natural organic matter is ubiquitous in aquatic systems (Gu et al., 2010; Jiang et al., 2015) and highly enhanced by solar radiation (Zheng and Hintelmann, 2009). However, this process is not likely to account for data observed in WJD due to the structure-specific reduction process of Hg(II) complexed by weakly bonding RO/N (e.g., carboxyl and amino) groups and the much stronger bonding RSH (e.g., thiol) group in DOM with time-dependent structural rearrangement (Jiang et al., 2015). Estimating the concentration of RSH to be equal to 0.15% × DOC mass (Skyllberg, 2008), or 0.5 μM of RSH at 10 mg. L^{-1} DOC, the highest RSH concentrations at the WJD site would be slightly greater than 1.3 μM, which indicates the RSH groups are not saturated by Hg(II). The Hg(II)/RSH ratio is much less than the optimum molar ratios (approximately 0.2×10^{-3}) of dark, Hg(II) abiotic reduction (Gu et al., 2010; Jiang et al., 2015). Thus, dark reduction processes can likely be discarded as being of major importance. Although MeHg microbial-degradation could be a contributor to the inverse correlation between MeHg and microbial-optical parameters (e.g., BIX) (Figs. S5–c), the relatively small log K_d (Fig. 7) may suggest that the negative relationship is more likely induced by bio-adsorption or accumulation resulting from the vigorous autochthonous activity (Machado et al., 2016). In WJD, the concentration of DTHg was positively correlated with both $SUVA_{254}$ (Fig. 8-e) and peak T (Figs. S5–d), suggesting that the DTHg variability was significantly related with DOM at WJD. DMeHg followed a similar pattern and was positively correlated with $SUVA_{254}$ (Figs. S5–e) but also with peak T (Fig. 8-f) and r(T/C) (Figs. S5–f). The correlation of DMeHg with $SUVA_{254}$ (Figs. S5–e) might denote on one hand an import of MeHg from the catchment to the lake (Herrero Ortega et al., 2017) and on the other hand the fact that specific terrestrial compounds might have also contributed to an enhanced MeHg production.

Previous works (Gerbig et al., 2011; Graham, 2013; Zhang et al., 2012, 2014) have demonstrated that highly aromatic DOM can stabilize the aggregation of HgS nano-particles, which in turn could be utilized by methylating bacteria. Also, higher aromaticity of DOM could enhance DMeHg released from the solid phase, lowering K_d, as observed in Fig. 7-d. High MeHg levels could be also explained by a higher MeHg production in WJD (Meng et al., 2010, 2016). Additionally, the possibility of DMeHg transported by DOM from allochthonous sources could be negligible. Because the sampling sites in this lake were far from the adjacent lands, and the land-use is mostly dryland, often in an oxic condition, the resulting relations between DMeHg and DOM is more likely explained by the within-lake (i.e., internal) process rather than runoff transportation (i.e., external). This explanation is also supported by the lack of positive correlation between DMeHg and DOM concentrations in this study (Fig. S2-c and S2-d). Therefore, the influences of DOM on Hg in WJD were more complicated than in CH and HF lake, with the mixture of both allochthonous and autochthonous DOM sources causing possible offsetting effects on solubility and net formation of MeHg.

3.7. Composition and bioavailability of DOM interplays with Hg speciation

The relationships between different DOM properties and Hg overall suggested that MeHg net formation in the lake sediments (i.e., HF and WJD) of this study, especially in WJD, is mainly driven by the activity of methylating microbes (Fig. 8-f, Fig. S4-a, b and Fig. S5-f). While other studies have reached similar conclusions (Kim et al., 2011; Mazrui et al., 2016), to our knowledge, only one study has measured, and thus linked, the bacterial activity to Hg methylation processes in sediments (Bravo et al., 2017). Bioavailability of DOM is dependent on DOM composition, the microbial community, and abundance (Yang et al., 2017). Thus, to confirm the role of the microbial activity, as indicated by DOM optical signatures and Hg methylation in sediments, we conducted a biodegradation incubation test for 16 days. To fit the kinetic process of biodegradation (Fig. 9), we assumed that the biodegradability of DOM in the collected sediment porewaters was decided by two distinct pools with different biodegradation rates, represented by labile and recalcitrant DOM fractions. The degradation was described by the following first-order kinetic model (Kalbitz et al., 2003; Wickland et al., 2007):

$$\text{Biodegraded DOM (\% of the original DOC)} = f_A(1\text{-}e^{-K1\times t}) + f_B(1\text{-}e^{-K2\times t}) \quad (4)$$

Where t is time (day), f_A is the percentage of labile DOM; f_B is the percentage of recalcitrant DOM, and K_1 and K_2 are the biodegradation rate constants for the two fractions of DOM, respectively. The sum of f_A and f_B is constrained to 1.0. We determined the half-

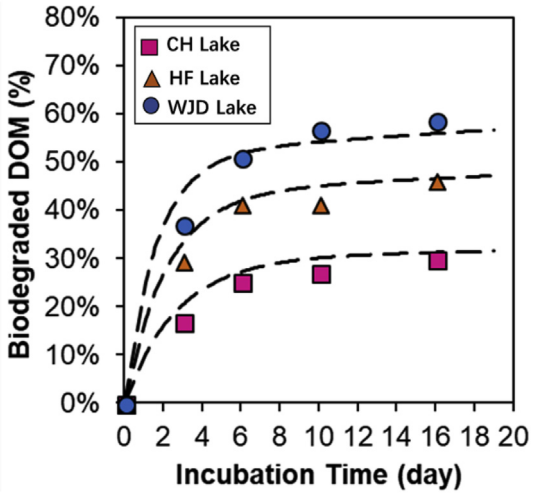

Fig. 9. Biodegradation kinetic curve of the porewater DOM from the three lake sediments. Black dash lines are the kinetic fitting curve of the first-order equation. Biodegraded DOM (%) was 0% at initial time (t_0).

Table 1
Biodegradation parameters of DOM in porewaters during a 16-day incubation experiment.[a]

Microbial source	Biodegradation capacity (%)[b]	$f_{A\ (\%)}$	$f_{B\ (\%)}$	K_1 (day^{-1})	K_2 (day^{-1})	Half-life of $f_{A\ (day)}$	Half-life of $f_{B\ (year)}$	Residence time (RT) of $f_{A\ (day)}$	Residence time (RT) of $f_{B\ (year)}$
CH	29.96	0.30	0.70	0.37	0.0012	1.87	1.64	2.70	2.36
HF	46.39	0.43	0.57	0.46	0.0036	1.51	0.53	2.17	1.67
WJD	58.91	0.51	0.49	0.60	0.0061	1.16	0.31	0.76	0.45

[a] Values reported in this table represent the means of at least duplicates. Sterile-filtered (0.22 μm Millipore filters) IHSS standard DOM samples (IHSS 1R105F Nordic Reservoir fulvic acid sample, 30 $mg.L^{-1}$) were inoculated with the indigenous microbial community solution in 100 ml blue-cap bottles with 25 ml headspace with N_2 (99.99%).
[b] Biodegradation capacity (%) is represented by the biodegraded DOM (% of the original DOC) calculated after a 16-day incubation.

life ($Ln2/K_i$) and average residence time ($1/K_i$) of the two pools, as reported in Table 1. Theoretically, for a given microbial community, labile (f_A) and recalcitrant (f_B) fractions of a DOM sample from a given site should be the constant. The different *f* values for different sampling sites (Table 1) may suggest that the microbial communities and their abilities to degrade DOM are totally different in the three studied reservoirs.

For a given DOM sample (i.e., the same sample), the microbial capacity to utilize DOM was greatest in WJD, with WJD > HF > CH (Table 1). The fastest biodegradation rate was likewise in WJD, while CH samples were slowest (Fig. 10). The highest microbial degradation capacity found in WJD is further evidenced by the microbial DOM optical signatures. As differences of microbial degradation capacities are generally attributed to the differences of microbial activities including either microbial composition/diversity or abundance (Reimers et al., 2013), a higher net Hg methylation observed in WJD could be attributed to enhanced microbial activity compared to CH and HF.

3.8. Limits and significances

Finally, the limitations of this study need to be emphasized. As a field investigation based on a limited number of samples, we hesitate to establish a general model for describing the variations of dissolved Hg species influenced by the DOM dynamics in lakes. The Hg cycling in aquatic systems is such a complex process controlled by many biogeochemical factors, in addition to DOM. We also recognize that lab-scale experiments designed to study mechanisms proposed here, as well as and larger-scale spatial-temporal field investigations are needed in order to develop such more generalized models. It also should be noted that DOM optical characterization can be influenced by concentration effects such as inner-filter effects (Gabor et al., 2014). Thus optical indices should be used with caution and similarly diluted DOM samples are recommended to be used when comparisons are made between waters of different regions.

With that stated, this study has demonstrated the importance of spectroscopic characteristics of DOM and we recommend these optical measurements be routinely incorporated into future environmental studies when assessing water quality and/or predicting potential risks of pollutants associated with DOM. Obviously, not all spectral parameters are informative in relation to the Hg cycle. This can in part be explained by the structural complexity of DOM resulting in a non-consistent pattern for some optical parameters (Kothawala et al., 2014; Hansen et al., 2016; Jiang et al., 2017a; b; Lescord et al., 2018). Because of this and the inherent heterogeneity of DOM, a combination of multiple methods (e.g., UV–Vis absorption plus fluorescence) is recommended for adequately assessing the role of DOM in the cycle of contaminants (Leenheer and Croué, 2003; Aiken et al., 2011a; b; Jiang et al., 2017b; Lescord et al., 2018).

4. Conclusion

Based on the spectral analysis of DOM, a mixing model consisting of two end-members of terrestrial and aquatic origins showed that porewater DOM characteristics in three Chinese lakes varied, from predominantly a terrestrial origin in the pristine lake (CH) to more algal- and microbial-derived DOM in the HF and WJD lakes. Our results highlight that while the relationships between DOC and Hg were inconsistent among lakes, DOM optical properties were useful in elucidating the sources of DOM and Hg. Furthermore, the often-reported correlations between DOC and Hg is concluded to be more likely observed in natural rather than anthropogenically influenced lakes. In the pristine CH lake, allochthonous DOM was more likely to bind Hg(II) but it was less able to provide energy for Hg methylating microorganisms. Labile DOM, from either autochthonous biological production or anthropogenic sources, seemed to drive microbial activity and resulted in high MeHg concentrations in the two most urban impacted reservoirs (WJD and HF). Three important highlights can be derived from

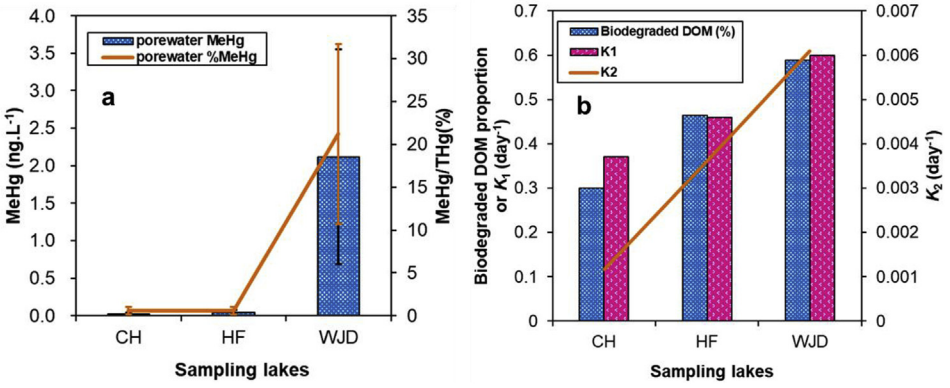

Fig. 10. Comparison of MeHg with DOM degradation parameters. WJD showed the highest MeHg level and net production (a), which also had the greatest microbial activities (b). The K_1 and K_2 are the biodegradation rate constants for the two fractions (i.e., labile vs. recalcitrant) of DOM, respectively.

this study (1) microbial activity reflected from fluorescence and absorption spectra of porewater DOM could help explain, in part, the variation in MeHg concentration in sediments and porewaters; (2) characterization of DOM composition could help explain the fate of Hg in environmental systems; (3) depending on the DOM composition, an increased DOM concentration might either result in high MeHg levels, transfer, and partition when DOM has a strong autochthonous signature or low MeHg levels when having terrestrial and recalcitrant signatures. Our results showed that beyond DOC concentrations, DOM properties helped to explain Hg cycling in the lake sediments and analyses of DOM composition should be considered in studies of Hg cycling in aquatic systems.

Acknowledgments

This work is financially supported by National Natural Science Foundation of China (41273099, 41403079), Sino-Swedish Mercury Management Research Framework (SMaRef) of Swedish Research Council (contract number D697801), and the National Key Basic Research Program of China (973 Program) (2013CB430004). Dr. Tao Jiang would personally thank Swedish Research Council to US (No. 621-2014-5370) for generously sponsoring his research position in Swedish University of Agricultural Sciences. Dr. Andrea G Bravo acknowledges the Generalitat de Catalunya (Beatriu de Pinos BP 00385–2016). Importantly, all authors want to thank the four anonymous reviewers for their valuable comments and suggestions to improve the reporting of this work.

Appendix A. Supplementary data

Supplementary data related to this article can be found at https://doi.org/10.1016/j.watres.2018.08.054.

References

Abbott, A.N., Haley, B.A., McManus, J., Reimers, C.E., 2015. The sedimentary flux of dissolved care earth elements to the ocean. Geochem. Cosmochim. Acta 154, 186–200.

Aiken, G.R., Gilmour, C.C., Krabbenhoft, D.P., Orem, W., 2011a. Dissolved organic matter in the Florida Everglades: implications for ecosystem restoration. Crit. Rev. Environ. Sci. Technol. 41, 217–248.

Aiken, G.R., Hsu-Kim, H., Ryan, J.N., 2011b. Influence of dissolved organic matter on the environmental fate of metals, nanoparticles, and colloids. Environ. Sci. Technol. 45, 3196–3201.

Asmala, E., Stedmon, C.A., Thomas, D.N., 2012. Linking CDOM spectral absorption to dissolved organic carbon concentrations and loadings in boreal estuaries. Estuar. Coast Shelf Sci. 111, 107–117.

Baker, A., 2001. Fluorescence excitation-emission matrix characterization of some sewage-impacted rivers. Environ. Sci. Technol. 35, 948–953.

Baker, A., 2002. Fluorescence properties of some farm wastes: implications for water quality monitoring. Water Res. 36, 189–195.

Baker, A., Cumberland, S.A., Bradley, C., Buckley, C., Bridgeman, J., 2015. To what extent can portable fluorescence spectroscopy be used in the real-time assessment of microbial water quality? Sci. Total Environ. 532, 14–19.

Bergamaschi, B.A., Krabbenhoft, D.P., Aiken, G.R., Patino, E., Rumbold, G.D., Orem, W.H., 2012. Tidally driven export of dissolved organic carbon, total mercury, and methylmercury from a mangrove-dominated estuary. Environ. Sci. Technol. 46, 1371–1378.

Birdwell, J.E., Engel, A.S., 2010. Characterization of dissolved organic matter in cave and spring waters using UV-Vis absorbance and fluorescence spectroscopy. Org. Geochem. 41, 270–280.

Birdwell, J.E., Valsaraj, K.T., 2010. Characterization of dissolved organic matter in fogwater by excitation-emission matrix fluorescence spectroscopy. Atmos. Environ. 44, 3246–3253.

Bolan, N.S., Adriano, D.C., Kunhikrishnan, A., James, T., McDowell, R., Senesi, N., 2011. Dissolved organic matter: biogeochemistry, dynamics, and environmental significance in soils. In: Sparks, D.L. (Ed.), Advances in Agronomy, vol. 110. Academic Press, Burlington, pp. 1–75.

Bravo, A.G., Bouchet, S., Tolu, J., Björn, E., Mateos-Rivera, A., Bertilsson, S., 2017. Molecular composition of organic matter controls methylmercury formation in boreal lakes. Nat. Commun. 8, 14255. https://doi.org/10.1038/ncomms14255.

Bravo, A.G., Kothawala, N.D., Attermeyer, K., Tessier, E., Bodmer, P., Ledesma, J.L.J., Audet, J., Pere Casas-Ruiz, J., Catalán, N., Cauvy-Fraunié, S., Colls, M., Deininger, A., Evtimova, V.V., Fonvielle, J.A., Fuß, T., Gilbert, P., Herrero Ortega, S., Liu, L., Mendoza-Lera, C., Monteiro, J., Mor, J.-R., Nagler, M., Niedrist, G.H., Nydahl, A.C., Pastor, A., Pegg, J., Robert, C.G., Pilotto, F., Portela, A.P., González-Quijano, C.R., Romero, F., Rulík, M., Amouroux, D., 2018. The interplay between total mercury, methlmercury and dissolved organic matter in fluvial systems: a latitudinal study across Europe. Water Res. 144, 172–182.

Burdige, D.J., Kline, S.W., Chen, W., 2004. Fluorescent dissolved organic matter in marine sediment pore waters. Mar. Chem. 89, 289–311.

Carstea, E.M., Bridgeman, J., Baker, A., Reynolds, D.M., 2016. Fluorescence spectroscopy for wastewater monitoring: a review. Water Res. 95, 205–219.

Chen, M., Hur, J., 2015. Pre-treatments, characteristics, and biogeochemical dynamics of dissolved organic matter in sediments: a review. Water Res. 79, 10–25.

Chiasson-Gould, S., Blais, J.M., Poulain, A.J., 2014. Dissolved organic matter kinetically controls mercury bioavailability to bacteria. Environ. Sci. Technol. 48, 3153–3161.

Clark, C.D., Aiona, P., Keller, J.K., De Bruyn, W.J., 2014. Optical characterization and distribution of chromophoric dissolved organic matter (CDOM) in soil porewater from a salt marsh ecosystem. Mar. Ecol. Prog. Ser. 516, 71–83.

Coble, P.G., 1996. Characterization of marine and terrestrial DOM in seawater using excitation-emission matrix spectroscopy. Mar. Chem. 51, 325–346.

Coble, P.G., 2007. Marine optical biogeochemistry: the chemistry of ocean color. Chem. Rev. 107, 402–418.

Coble, P.G., Spencer, R.G.M., Baker, A., Reynolds, D.M., 2014. Aquatic organic matter fluorescence. In: Coble, P.G., Lead, J., Baker, A., Reynolds, D.M., Spencer, R.G.M. (Eds.), Aquatic Organic Matter Fluorescence. Cambridge University Press. US, pp. 75–122.

Dang, D.H., Lenoble, V., Durrieu, G., Mullot, J.-U., Mounier, S., Garnier, C., 2014. Sedimentary dynamics of coastal organic matter: an assessment of the porewater size/reactivity model by spectroscopic techniques. Estuar. Coast Shelf Sci. 151, 100–111.

Dittman, J.A., Shanley, J.B., Driscoll, C.T., Aiken, G.R., Chalmers, A.T., Towse, J.E., 2009. Ultraviolet absorbance as a proxy for total dissolved mercury in streams. Environ. Pollut. 157, 1953–1956.

Driscoll, C.T., Blette, V., Yan, C., Schofield, C.L., Munson, R., Holsapple, J., 1995. The role of dissolved organic carbon in the chemistry and bioavailability of mercury in remote Adirondack lakes. Water Air Soil Pollut. 80, 499–508.

Drott, A., Lambertsson, L., Björn, E., Skyllberg, U., 2008. Do potential methylation rates reflect accumulated methyl mercury in contaminated sediments? Environ. Sci. Technol. 42, 153–158.

Eckley, C.S., Watras, C.J., Hintelmann, H., Morrison, K., Kent, A.D., Regnell, O., 2005. Mercury methylation in the hypolimnetic waters of lakes with and without connection to wetlands in northern Wisconsin. Can. J. Fish. Aquat. Sci. 411, 400–411.

Eklöf, K., Fölster, J., Sonesten, L., Bishop, K., 2012. Spatial and temporal variation of THg concentrations in run-off water from 19 boreal catchments, 2000-2010. Environ. Pollut. 164, 102–109.

Fasching, C., Behounek, B., Singer, G.A., Battin, T.J., 2014. Microbial degradation of terrigenous dissolved organic matter and potential consequences for carbon cycling in brown-water streams. Sci. Rep. 4, 4981. https://doi.org/10.1038/srep04981.

Fellman, J.B., Hood, E., D'Amore, D.V., Edwards, R.T., White, D., 2009. Seasonal changes in the chemical quality and biodegradability of dissolved organic matter exported from soils to streams in coastal temperate rainforest watershed. Biogeochemistry 95, 277–293.

Fellman, J.B., Hood, E., Spencer, R.G.M., 2010. Fluorescence spectroscopy opens new windows into dissolved organic matter dynamics in freshwater ecosystems: a review. Limnol. Oceanogr. 55, 2452–2462.

Feng, C., Yan, H., Yu, B., Li, Q., 2012. Influence of cage culture on methylmercury in water column of reservoir (In Chinese with English Abstract). Chin. J. Ecol. 1438–1446.

Fichot, C.G., Benner, R., 2012. The spectral slope coefficient of chromophoric dissolved organic matter ($S_{275-295}$) as a tracer of terrigenous dissolved organic carbon in river influenced ocean margins. Limnol. Oceanogr. 57, 1453–1466.

Fichot, C.G., Kaiser, K., Hooker, S.B., Amon, R.M.W., Babin, M., Bélanger, S., Walker, S.A., Benner, R., 2013. Pan-Arctic distributions of continental runoff in the Arctic Ocean. Sci. Rep. 3, 1053. https://doi.org/10.1038/srep01053.

Förstner, U., 2004. Sediment dynamics and pollutant mobility in rivers: an interdisciplinary approach. Lake Reservoir Manag. 9, 25–40.

Fu, P., Kawamura, K., Chen, J., Qin, M., Ren, L., Sun, Y., Wang, Z., Barrie, L.A., Tachibana, E., Ding, A., Yamashita, Y., 2015. Fluorescent water-soluble organic aerosols in the High Arctic atmosphere. Sci. Rep. 5, 9845. https://doi.org/10.1038/srep09845.

Gabor, R.S., Baker, A., McKnight, D.M., Miller, M.P., 2014. Fluorescence indices and their interpretation. In: Coble, P.G., Lead, J., Baker, A., Reynolds, D.M., Spencer, R.G.M. (Eds.), Aquatic Organic Matter Fluorescence. 2014. Cambridge University Press, US, pp. 303–338.

Galapate, R.P., Baes, A.U., Ito, K., Mukai, T., Shoto, E., Okada, M., 1998. Detection of domestic wastes in Kurose river using synchronous fluorescence spectroscopy. Water Res. 32, 2232–2239.

Gascón Díez, E., Loizeau, J.-L., Cosio, C., Bouchet, S., Adatte, T., Amouroux, D., Bravo, A.G., 2016. Role of settling particles on mercury methylation in the oxic water column of freshwater systems. Environ. Sci. Technol. 50, 11672–11679.

Gerbig, C.A., Kim, C.S., Stegemeier, J.P., Ryan, J.N., Aiken, G.R., 2011. Formation of nanocolloidal metacinnabar in mercury-DOM-sulfide systems. Environ. Sci. Technol. 45, 9180–9187.

Gerbig, C.A., Ryan, J.N., Aiken, G.R., 2012. The effects of dissolved organic matter on mercury biogeochemistry. In: Liu, G., Cai, Y., O'Driscoll, N. (Eds.), Environmental Chemistry and Toxicology of Mercury. John Wiley & Sons. US, pp. 259–292.
Gilmour, C.C., Podar, M., Bullock, A.L., Graham, A.M., Brown, S.D., Somenahally, A.C., Johs, A., Hurt Jr., R.A., Bailey, K.L., Elias, D.A., 2013. Mercury methylation by novel microorganisms from new environments. Environ. Sci. Technol. 47, 11810–11820.
Graham, A.M., Aiken, G.R., Gilmour, C.C., 2012. Dissolved organic matter enhances microbial mercury methylation under sulfidic conditions. Environ. Sci. Technol. 46, 2715–2723.
Graham, A.M., Aiken, G.R., Gilmour, C.C., 2013. Effect of dissolved organic matter source and character on microbial Hg methylation in Hg-S-DOM solutions. Environ. Sci. Technol. 47, 5746–5754.
Gu, B., Bian, Y., Miller, C.L., Dong, W., Jiang, X., Liang, L., 2010. Mercury reduction and complexation by natural organic matter in anoxic environments. Proc. Natl. Acad. Sci. Unit. States Am. 108 (4), 1479–1483.
Guillemette, F., Wachenfeldt, E.V., Kothawala, D.N., Bastviken, D., Tranvik, L.J., 2017. Preferential sequestration of terrestrial organic matter in boreal lake sediments. J. Geophys. Res. Biogeosci. 122, 863–874. https://doi.org/10.1002/2016JG003735.
Hammerschmidt, C.R., Fitzgerald, W.F., 2004. Geochemical controls on the production and distribution of methylmercury in near-shore marine sediments. Environ. Sci. Technol. 38, 1487–1495.
Hammerschmidt, C.R., Fitzgerald, W.F., Balcom, P.H., Visscher, P.T., 2008. Organic matter and sulfide inhibit methylmercury production in sediments of New York/New Jersey Harbor. Mar. Chem. 109, 165–182.
Hansen, A.M., Kraus, T.E.C., Pellerin, B.A., Fleck, J.A., Downing, B.D., Bergamaschi, B.A., 2016. Optical properties of dissolved organic matter (DOM): effects of biological and photolytic degradation. Limnol. Oceanogr. 61, 1015–1032.
He, T., Wu, Y., Feng, X., 2010. The impact of eutrophication on distribution and speciation of mercury in Hongfeng Reservoir, Guizhou Province (In Chinese with English abstract). J. Lake Sci. 22, 208–214.
He, W., Jun, H., Lee, J.-H., Hur, J., 2016. Difference in spectroscopic characteristics between dissolved and particulate organic matters in sediments: insight into distribution behavior of sediment organic matter. Sci. Total Environ. 547, 1–8.
Helms, J.R., Stubbins, A., Ritchie, J.D., Minor, E.C., Kieber, D.J., Mopper, K., 2008. Absorption spectral slopes and slope ratios as indicators of molecular weight, source, and photobleaching of chromophoric dissolved organic matter. Limnol. Oceanogr. 53, 955–969.
Herrero Ortega, S., Catalán, N., Björn, E., Gröntoft, H., Hilmarsson, T.G., Bertilsson, S., Wu, P., Bishop, K., Levanoni, O., Bravo, A.G., 2017. High methylmercury formation in ponds fueled by fresh humic and algal derived organic matter. Limnol. Oceanogr. 63, S44–S53.
Hsu-Kim, H., Kucharzyk, K.H., Zhang, T., Deshusses, M.A., 2013. Mechanisms regulating mercury bioavailability for methylating microorganisms in the aquatic environment: a critical review. Environ. Sci. Technol. 47, 2441–2456.
Huguet, A., Vacher, L., Relexans, S., Saubusse, S., Froidefond, J.M., Parlanti, E., 2009. Properties of fluorescent dissolved organic matter in the Gironde Estuary. Org. Geochem. 40, 706–719.
Hurley, J.P., Krabbenhoft, D.P., Cleckner, L.B., Olson, M.L., Aiken, G.R., Rawlik, P.S., 1998. System controls on the aqueous distribution of mercury in the northern Florida Everglades. Biogeochemistry 40, 293–310.
Isidorova, A., Bravo, A.G., Riise, G., Bouchet, S., Björn, E., Sobek, S., 2016. The effect of lake browning and respiration mode on the burial and fate of carbon and mercury in the sediment of two boreal lakes. J. Geophys. Res. Biogeosci. 121, 233–245. https://doi.org/10.1002/2015JG003086.
Jiang, T., Skyllberg, U., Wei, S., Wang, D., Lu, S., Jiang, Z., Flanagan, D.C., 2015. Modelling of the structure-specific kinetics of abiotic, dark reduction of Hg(II) complexed by O/N and S functional groups in humic acids while accounting for time-dependent structural rearrangement. Geochem. Cosmochim. Acta 154, 151–167.
Jiang, T., Skyllberg, U., Björn, E., Green, N.W., Tang, J., Wang, D., Gao, J., Li, C., 2017a. Characteristics of dissolved organic matter (DOM) and relationship with dissolved mercury in Xiaoqing River-Laizhou Bay estuary, Bohai Sea, China. Environ. Pollut. 223, 19–30.
Jiang, T., Kaal, J., Liang, J., Zhang, Y., Wei, S., Wang, D., Green, N.W., 2017b. Composition of dissolved organic matter (DOM) from periodically submerged soils in the Three Gorges Reservoir areas as determined by elemental and optical analysis, infrared spectroscopy, pyrolysis-GC–MS and thermally assisted hydrolysis and methylation. Sci. Total Environ. 603–604, 461–471.
Jiang, T., Chen, X., Wang, D., Liang, J., Bai, W., Zhang, C., Wang, Q., Wei, S., 2018a. Dynamics of dissolved organic matter (DOM) in a typical inland lake of the Three Gorges Reservoir area: fluorescent properties and their implications for dissolved mercury species. J. Environ. Manag. 206, 418–429.
Jiang, T., Wang, D., Wei, S., Yan, J., Liang, J., Chen, X., Liu, J., Wang, Q., Lu, S., Gao, J., Li, L., Guo, N., Zhao, Z., 2018b. Influences of the alternation of wet-dry periods on the variability of chromophoric dissovled organic matter in the water level fluctuation zone of the Three Gorges Reservoir area, China. Sci. Total Environ. 636, 249–259.
Jonsson, S., Skyllberg, U., Nilsson, M.B., Westlund, P.-O., Shchukarev, A., Lundberg, E., Björn, E., 2012. Mercury methylation rates for geochemically relevant Hg(II) species in sediments. Environ. Sci. Technol. 46, 11653–11659.
Jonsson, S., Skyllberg, U., Nilsson, M.B., Lundberg, E., Andersson, A., Björn, E., 2014. Differentiated availability of geochemical mercury pools controls methylmercury levels in estuarine sediment and biota. Nat. Commun. 5, 4624. https://doi.org/10.1038/ncomms5624.
Kalbitz, K., Schmerwitz, J., Schwesig, D., Matzner, E., 2003. Biodegradation of soil-derived dissolved organic matter as related to its properties. Geoderma 113, 273–291.
Kappler, A., Benz, M., Schink, B., Brune, A., 2004. Electron shuttling via humic acids in microbial iron(III) reduction in a freshwater sediment. FEMS (Fed. Eur. Microbiol. Soc.) Microbiol. Ecol. 47, 85–92.
Kim, M., Han, S., Gieskes, J., Deheyn, D.D., 2011. Importance of organic matter lability for monomethylmercury production in sulfate-rich marine sediments. Sci. Total Environ. 409, 778–784.
Kim, H., Soerensen, A.L., Hur, J., Heimbürger, L.-E., Hahm, D., Rhee, T.S., Noh, S., Han, S., 2017. Methylmercury mass budgets and distribution characteristics in the Western Pacific ocean. Environ. Sci. Technol. 51, 1186–1194.
Kothawala, D.N., Von Wachenfeldt, E., Koehler, B., Tranvik, L.J., 2012. Selective loss and preservation of lake water dissolved organic matter fluorescence during long-term dark incubations. Sci. Total Environ. 433, 238–246.
Kothawala, D.N., Stedmon, C.A., Müller, R.A., Weyhenmeyer, G.A., Köhler, S.J., Tranvik, L.J., 2014. Controls of dissolved organic matter quality:evidence from a large-scale boreal lake survey. Global Change Biol. 20, 1101–1114.
Lavoie, R.A., Jardine, T.D., Chumchal, M.M., Kidd, K.A., Campbell, L.M., 2013. Biomagnification of mercury in aquatic food webs: a world wide meta-analysis. Environ. Sci. Technol. 47, 13385–13394.
Leenheer, J.A., Croué, J.P., 2003. Characterizing dissolved aquatic organic matter. Environ. Sci. Technol. 37, 18A–26A.
Lehnherr, I., 2014. Methylmercury biogeochemistry: a review with special reference to Arctic aquatic ecosystems. Environ. Rev. 22, 229–243.
Lescord, G.L., Emilson, E.J.S., Johnston, T.A., Branfireun, B.A., Gunn, J.M., 2018. Optical properties of dissolved organic matter and their relation to mercury concentrations in water and biota across a remote freshwater drainage basin. Environ. Sci. Technol. 52, 3344–3353.
Logue, J.B., Stedomn, C.A., Kellerman, A.M., Nielsen, N.J., Andersson, A.F., Laudon, H., Lindström, E.S., Kritzberg, E.S., 2016. Experimental insights into the importance of aquatic bacterial community composition to the degradation of dissolved organic matter. ISME J. 10, 533–545.
Machado, W., Sanders, C.J., Santos, I.R., Sanders, L.M., Silva-Filho, E.V., Luiz-Silva, W., 2016. Mercury dilution by autochthonous organic matter in a fertilized mangrove wetland. Environ. Pollut. 213, 30–35.
Mazrui, N.M., Jonsson, S., Thota, S., Zhao, J., Mason, R.P., 2016. Enhanced availability of mercury bound to dissolved organic matter for methylation in marine sediments. Geochem. Cosmochim. Acta 194, 153–162.
McKnight, D.M., Boyer, E.W., Westerhoff, P.K., Doran, P.T., Kulbe, T., Anderson, D.T., 2001. Spectrofluorometric characterization of dissolved organic matter for identification of precursor material and aromaticity. Limnol. Oceanogr. 46, 38–48.
Meng, B., Feng, X.B., Chen, C.X., Qiu, G.L., Sommar, J., Guo, Y.N., Liang, P., Wan, Q., 2010. Influence of eutrophication on the distribution of total mercury and methylmercury in hydroelectric reservoirs. J. Environ. Qual. 39, 1624–1635.
Meng, B., Feng, X., Qiu, G., Li, Z., Yao, H., Shang, L., Yan, H., 2016. The impacts of organic matter on the distribution and methylation of mercury in a hydroelectric reservoir in Wujiang River, Southwest China. Environ. Toxicol. Chem. 35, 191–199.
Mierle, G., Ingram, R., 1991. The role of humic substances in the mobilization of mercury from watersheds. Water Air Soil Pollut. 56, 349–357.
Mopper, K., Kieber, D.J., Stubbins, A., 2015. Marine photochemistry of organic matter: processes and impacts (Chapter 8). In: Hansell, D.A., Carlson, C.A. (Eds.), Biogeochemistry of Marine Dissolved Organic Matter. Academic Press. Elsevier, UK, pp. 389–450.
Mostofa, K.M.G., Liu, C., Mottaleb, M.A., Wan, G., Ogawa, H., Vione, D., Yoshioka, T., Wu, F., 2013. Dissolved organic matterin natural waters (Chapter 1). In: Mostofa, K.M.G., Yoshioka, T., Mottaleb, A., Vione, D. (Eds.), Photobiogeochemistry of Organic Matter: Principles and Practices in Water Environments. Springer, Berlin, pp. 1–137.
Nelson, N.B., Siegel, D.A., 2013. The global distribution and dynamics of chromophoric dissolved organic matter. Ann. Rev. Mar. Sci. 5, 447–476.
Noh, S., Kim, J., Hur, J., Hong, Y., Han, S., 2018. Potential contributions of dissolved organic matter to monomethylmercury distributions in temperate reservoirs as revealed by fluorescence spectroscopy. Environ. Sci. Pollut. Res. 25, 6474–6486.
Nowicki, S., Lapworth, D.J., Ward, J.S.T., Thomson, P., Charles, K., 2019. Tryptophan-like fluorescence as a measure of microbial contamination risk in groundwater. Sci. Total Environ. 646, 782–791.
Old, G.H., Naden, P.S., Granger, S.J., Bilotta, G.S., Brazier, R.E., Macleod, C.J.A., Krueger, T., Bol, R., Hawkins, J.M.B., Haygarth, P., Freer, J., 2012. A novel application of natural fluorescence to understand the sources and transport pathways of pollutants from livestock farming in small headwater catchments. Sci. Total Environ. 417–418, 169–182.
Parks, J.M., Johs, A., Podar, M., Bridou, R., Hurt Jr., R.A., Smith, S.D., Tomanicek, S.J., Qian, Y., Brown, S.D., Brandt, C.C., Palumbo, A.V., Smith, J.C., Wall, J.D., Elias, D.A., Liang, L., 2013. The genetic basis for bacteria mercury methlation. Science 339, 1332–1335.
Perdue, E.M., Koprivnjak, J.-F., 2007. Using the C/N ratio to estimate terrigenous inputs of organic matter to aquatic environment. Estuar. Coast Shelf Sci. 73 (1–2), 65–72.
Peretyazhko, T., Sposito, G., 2006. Reducing capacity of terrestrial humic acids. Geoderma 137, 140–146.

Pickhardt, P.C., Folt, C.L., Chen, C.Y., Klaue, B., Blum, J.D., 2002. Algal blooms reduce the uptake of toxic methylmercury in freshwater food webs. Proc. Natl. Acad. Sci. Unit. States Am. 99, 4419–4423.
Qian, X.L., Feng, X.B., Bi, X.Y., He, T.R., Guo, Y.N., Fu, X.W., Li, P., 2008. Concentrations and distributions of mercury species in surface water and pore water of Lake Caohai, Guizhou Province. (In Chinese, with English abstract. J. Lake Sci. 20, 563–570.
Ravichandran, M., 2004. Interaction between mercury and dissolved organic matter-a review. Chemosphere 55, 319–331.
Reddy, K.R., Delaune, R.D. (Eds.), 2008. Biogeochemistry of Wetlands: Science and Application. CRC Press, US, pp. 141–151.
Reimers, C.E., Alleau, Y., Bauer, J.E., Delaney, J., Girguis, P.R., Schrader, P.S., Stercher III, H.A., 2013. Redox effects on the microbial degradation of refractory organic matter in marine sediments. Geochem. Cosmochim. Acta 121, 582–598.
Rochelle-Newall, E.J., Fisher, T.R., 2002. Chromophoric dissolved organic matter and dissolved organic carbon in Chesapeake Bay. Mar. Chem. 77, 23–41.
Schartup, A.T., Mason, R.P., Balcom, P.H., Hollweg, T.A., Chen, C.Y., 2013. Methylmercury production in estuarine sediments: role of organic matter. Environ. Sci. Technol. 47, 695–700.
Senesi, N., Xing, B., Huang, P.M. (Eds.), 2009. Biophysico-chemical Processes Involving Natural Nonliving Organic Matter in Environmental Systems. John Wiley & Sons, US.
Shang, L., Li, Q., Qiu, H., Qiu, G., Li, G., Feng, X., 2011. Chlorophyll-a distribution and phosphorus cycle in water body of Hongfeng Reservoir, Guizhou (In Chinese with English Abstract). Chin. J. Eco 30, 1023–1030.
Skyllberg, U., 2008. Competition among thiol and inorganic sulfides and polysulfides for Hg and MeHg in wetland soils and sediments under suboxic conditions: illumination of controversies and implications for MeHg net production. J. Geophys. Res. Biogeosci. 113, G00C03. https://doi.org/10.1029/2008JG000745.
Skyllberg, U., 2012. Chemical speciation of mercury in soil and sediment. In: Liu, G., Cai, Y., O'Driscoll, N. (Eds.), Environmental Chemistry and Toxicology of Mercury. John Wiley & Sons, US, pp. 219–258.
Sorensen, J.P.R., Baker, A., Cumberland, S.A., Lapworth, D.J., MacDonald, A.M., Pedley, S., Taylor, R.G., Ward, J.S.T., 2018a. Real-time detection of faecally contaminated drinking water with tryptophan-like fluorescence: defining threshold values. Sci. Total Environ. 622–623, 1250–1257.
Sorensen, J.P.R., Vivanco, A., Ascott, M.J., Gooddy, D.C., Lapworth, D.J., Read, D.S., Rushworth, C.M., Bucknall, J., Herbert, K., Karapanos, I., Gumm, L.P., Taylor, R.G., 2018b. Online fluorescence spectroscopy for the real-time evaluation of the microbial quality of drinking water. Water Res. 137, 301–309.
Spencer, R.G.M., Butler, K.D., Aiken, G.R., 2012. Dissolved organic carbon and chromophoric dissolved organic properties of rivers in the USA. J. Geophys. Res. Biogeosci. 117, G03001. https://doi.org/10.1029/2011JG001928.
Tfaily, M.M., Hamdan, R., Corbett, J.E., Chanton, J.P., Glaser, P.H., Cooper, W.T., 2013. Investigation dissolved organic matter decomposition in northern peatland using complimentary analytical techniques. Geochem. Cosmochim. Acta 112, 116–129.
Tjerngren, I., Meili, M., Björn, E., Skyllberg, U., 2012a. Eight boreal wetlands as sources and sinks for methyl mercury in relation to soil acidity, C/N ratio, and small-scale flooding. Environ. Sci. Technol. 46, 8052–8060.
Tjerngren, I., Karlsson, T., Björn, E., Skyllberg, U., 2012b. Potential Hg methylation and MeHg demethylation rates related to the nutrient status of different boreal wetlands. Biogeochemistry 108, 335–350.
Tranvik, L.J., Downing, J.A., Cotner, J.B., Loiselle, S.A., Striegl, R.G., Ballatore, T.J., Dillon, P., Finlay, K., Fortino, K., Knoll, L.B., Kortelainen, P.L., Kutser, T., Larsen, S., Laurion, I., Leech, D.M., McCallister, S.L., McKnight, D.M., Melack, J.M., Overholt, E., Porter, J.A., Prairie, Y., Renwick, W.H., Roland, F., Sherman, B.S., Schindler, D.W., Sobek, S., Tremblay, A., Vanni, M.j., Verschoor, A.M., von Wachenfeldt, E., Weyhenmeyer, G.A., 2009. Lakes and reservoirs as regulators of carbon cycling and climate. Limnol. Oceanogr. 54, 2298–2314.
Waples, J.S., Nagy, K.L., Aiken, G.R., Ryan, J.N., 2005. Dissolution of cinnabar (HgS) in the presence of natural organic matter. Geochem. Cosmochim. Acta 69, 1575–1588.
Weishaar, J.L., Aiken, G.R., Bergamaschi, B.A., Fram, M.S., Fujii, R., Mopper, K., 2003. Evaluation of specific ultraviolet absorbance as an indicator of the chemical composition and reactivity of dissolved organic carbon. Environ. Sci. Technol. 37, 4702–4708.
Wickland, K.P., Neff, J.C., Aiken, G.R., 2007. Dissolved organic carbon in Alaskan boreal forest: sources, chemical characteristics, and biodegradability. Ecosystem 10, 1323–1340.
Wilson, H.F., Xenopoulos, M.A., 2009. Effects of agricultural land use on the composition of fluvial dissolved organic matter. Nat. Geosci. 2, 37–41.
Yan, H., Li, Q., Meng, B., Wang, C., Feng, X., He, T., Dominik, J., 2013. Spatial distribution and methylation of mercury in a eutrophic reservoir heavily contaminated by mercury in Southwest China. Appl. Geochem. 33, 182–219.
Yang, L., Hur, J., 2014. Critical evaluation of spectroscopic indices for organic matter source tracing via end member mixing analysis based on two contrasting sources. Water Res. 59, 80–89.
Yang, L., Zhuang, W.-E., Chen, C.-T.A., Wang, B.-J., Kuo, F.-W., 2017. Unveiling the transformation and bioavailability of dissolved organic matter in contrasting hydrothermal vents using fluorescence EEM-PARAFAC. Water Res. 111, 195–203.
Zhang, Y.L., Qin, B.Q., Chen, W.M., Zhu, G.W., 2005. A preliminary study of chromophoric dissolved organic matter (CDOM) in Lake Taihu, a shallow subtropical lake in China. Clean (Weinh) 33, 315–323.
Zhang, T., Kim, B., Levard, C., Reinsch, B.C., Lowry, G.V., Deshusses, M.A., Hsu-Kim, H., 2012. Methylation of mercury by bacteria exposed to dissolved, nanoparticulate, and microparticulate mercuric sulfides. Environ. Sci. Technol. 46, 6950–6958.
Zhang, T., Kucharzyk, K.H., Kim, B., Deshusses, M.A., Hsu-Kim, H., 2014. Net methylation of mercury in Estuarine sediment microcosms amended with dissolved, nanoparticulate, and microparticulate mercuric sulfides. Environ. Sci. Technol. 48, 9133–9141.
Zhao, L., Guo, Y., Meng, B., Yao, H., Feng, X., 2017. Effects of damming on the distribution and methylation of mercury in Wujiang River, Southwest China. Chemosphere 185, 780–788.
Zheng, W., Hintelmann, H., 2009. Mercury isotope fractionation during photoreduction in natural water is controlled by its Hg/DOC ratio. Geochim. Cosmochim. Acta. 73, 6704–6715.
Zhou, Y., Jeppesen, E., Zhang, Y., Niu, C., Shi, K., Liu, X., Zhu, G., Qin, B., 2015. Chromophoric dissolved organic matter of black waters in a highly eutrophic Chinese lake: freshly produced from algal scums. J. Hazard Mater. 299, 222–230.
Zhou, Y., Shi, K., Zhang, Y., Jeppesen, E., Liu, X., Zhou, Q., Wu, H., Tang, X., Zhu, G., 2017. Fluorescence peak integration ratio IC:IT as a new potential indicator tracing the compositional changes in chromophoric dissolved organic matter. Sci. Total Environ. 574, 1588–1598.
Ziegelgruber, K.L., Zeng, T., Arnold, W.A., Chin, Y.-P., 2013. Sources and composition of sediment pore-water dissolved organic matter in prairie pothole lakes. Limnol. Oceanogr. 58, 1136–1146.